ELSEVIER

Catalysis Today 83 (2003) 19–31

CATALYSIS TODAY

www.elsevier.com/locate/cattod

Premixed metal fibre burners based on a Pd catalyst

Isotta Cerri*, Matteo Pavese, Guido Saracco, Vito Specchia

Dipartimento di Scienza dei Materiali e Ingegneria Chimica, Politecnico di Torino, Corso Duca degli Abruzzi 24, 10129 Turin, Italy

Received 1 May 2002; received in revised form 28 November 2002; accepted 18 March 2003

Abstract

As an alternative to previously developed catalytic FeCrAlloy fibre mat burners based on perovskite catalysts, new catalytic burners have been developed based on Pd catalyst on lantana-stabilised Al_2O_3 and different fibre structures (NIT100A, NIT100S and NIT200S by ACOTECH NV). All development steps are considered, shifting from catalyst preparation (based on combustion synthesis of γ-Al_2O_3) to the optimisation of lantana and Pd loadings, from the definitions of the best catalyst-deposition conditions (washcoating) to the catalytic burners performances, determined in an ad hoc developed combustion chamber. The results show almost half pollutants emissions and better performance compared to various non-catalytic counterparts, especially as far as CO and NO_x emissions are concerned. Some flame instability problems were though registered, especially for one of the catalytic burner mattresses employed, at low specific power inputs and excesses of air ($<375\,kW/m^2$ and $<12\%$, respectively). Further, PdO/Pd transition is shown to influence the dynamic behaviour of the catalytic burners.

Keywords: FeCrAlloy fibre burners; Catalytic combustion; Pd–Al_2O_3; Natural gas; Washcoating; Combustion synthesis

1. Introduction

In line with the modern climate policies, internationally defined to reduce the greenhouse gas generation [1], new advanced natural gas premixed combustion systems based on porous media burners with enhanced energy efficiency and low environmental impact (reduction of the greenhouse gas CO_2, the toxic gases CO, NO_x and unburned hydrocarbons—HC) are being extensively developed [2–11].

In premixed porous burners supplied with natural gas, the flame front dynamically stabilises at the balance position where the laminar flame speed equals the supplied gas speed [12,13]. At low thermal power and air-to-fuel ratio, since the gas speed is lower than the adiabatic combustion speed the flame moves upstream toward the burner that emits most of the heat as thermal radiation. The solid plays the role of cooling the flame, and the flame speed decreases until approaching the unburned gas speed; the combustion results partly stabilized in a thin layer within the burner and near the downstream surface (*radiant regime*). Conversely, by increasing the gas flow rate, the flame is progressively blown-off the burner surface, until the occurrence of the *blue-flame regime*, characterised by a 'carpet' of short blue flames all immediately close to the cold downstream surface. The heat is less intensively transferred by convection leading to higher flame temperatures, responsible for higher thermal NO_x emissions (even though they remain lower than those generated by diffusive flames). At intermediate values of the excess air and thermal power, a third regime named

* Corresponding author. Tel.: +39-011-5644-710; fax: +39-011-5644-699.
E-mail address: cerri@athena.polito.it (I. Cerri).

0920-5861/$ – see front matter
doi:10.1016/S0920-5861(03)00213-X

transition regime, occurs. This regime is characterised by the simultaneous presence of little blue-flame and radiant zones over the firing surface.

The present contribution is aimed at developing a catalytic burner to be assembled in a low emissions domestic boiler (maximum thermal power of about 25 kW), capable of modulating the thermal power with a large turndown ratio (eventually 10:1) according to the users' load request from a minimum power of 2–3 kW (needed for house heating) up to a maximum power of about 25 kW (enabling a rapid production hot water for domestic use). A power modulating control system, rather than the on–off based one, is generally recognised as the best way of drastically cutting down undesired pollutants peaks, quick material degradation and energy loss occurring during on–off transients.

The catalyst has to guarantee very low pollutant emissions even at low combustion temperatures. For this purpose, a suitable catalyst should combine good activity towards methane combustion in the temperature range 600–1100 °C with high thermal stability. Palladium supported on stabilized alumina has been found to be the most promising catalytic system for the complete oxidation of methane, especially when catalytic ignition is pursued [14]. In spite of the intensive research on the Pd/alumina system, there is still a remarkable divergence of opinions concerning, for instance, the Pd/PdO redox mechanism during reaction, or the kinetic mechanisms, or even about the most active catalyst state for high temperature methane oxidation [15,16]. It is generally recognised that Pd-metal is less active in methane combustion at temperature lower than approximately 800 °C; however discussions are still open about the more active state of PdO_x, i.e. Pd with chemisorbed oxygen [17], Pd-particle with a skin of PdO [18] or bulk PdO [19]. On the basis of the extensive literature data, it seemed not useful to attempt at stabilising palladium in the PdO form for the present application, where active catalysts for high-temperature combustion (even above 800 °C) are pursued, and the metallic state of Pd is indicated as the stable one.

Catalytic burners based on a FeCrAlloy fibre mat support and a Pd/alumina catalyst were developed and tested in a specific pilot plant; this allowed to set a comparison with earlier studies on pervoskite-catalysed fibre burners [8–10] showing the superior performance of the noble-metal based catalytic burners, despite stability problems (i.e. increased flashback tendency) were detected for these Pd-based burners and, to some extent, analysed.

2. Experimental

2.1. The knitted fibre supports: optimised pretreatment

The virgin non-catalytic burners considered in the present study are three metal fibre panels commercialised by NV Acotech SA (Zwevegem, Belgium): NIT100A, NIT100S and NIT200S (in the following referred as products A, B and C, respectively), made of FeCrAlloy, a high thermal resistance alloy, (with Al content about 5 wt.%). At high temperature Al diffuses towards the alloy surface where it is oxidised to α-alumina, thus generating a protecting coating layer, preventing from further oxidation of iron or chromium and undesired alloy degradation [20]. In the three commercial products, a yarn of fine FeCrAlloy fibres (fibre diameter about 35–45 μm) is knitted to form the textile products different in the nominal thickness and density, as shown in Table 1. The lower the density and thickness the lower the price per unit surface, and consequently the burner mat durability. Product C was taken into account due to the expected longer life, while product A because of the lower market price. Product B was selected and more deeply investigated because it appeared as a potential compromise of the previous two, by providing a satisfying long term resistance at an acceptable cost [21].

After a conventional 1 h thermal treatment at 900 °C in still air [20], the alumina oxide layer presents a globular morphology, not completely suitable for anchoring deposited layers. In order to get an alumina layer, strictly anchored to the basic alloy and with a rough external surface, a pre-oxidation treatment was

Table 1
Basic properties of the metal fibre mats used in the present investigation (bulk FeCrAlloy density: 7220 kg/m^3)

Product	Trade name	Thickness (mm)	Density (kg/m^2)
A	NIT100A	1.4	0.6–0.8
B	NIT100S	2.2	1.2–1.4
C	NIT200S	3.1	2.2–2.4

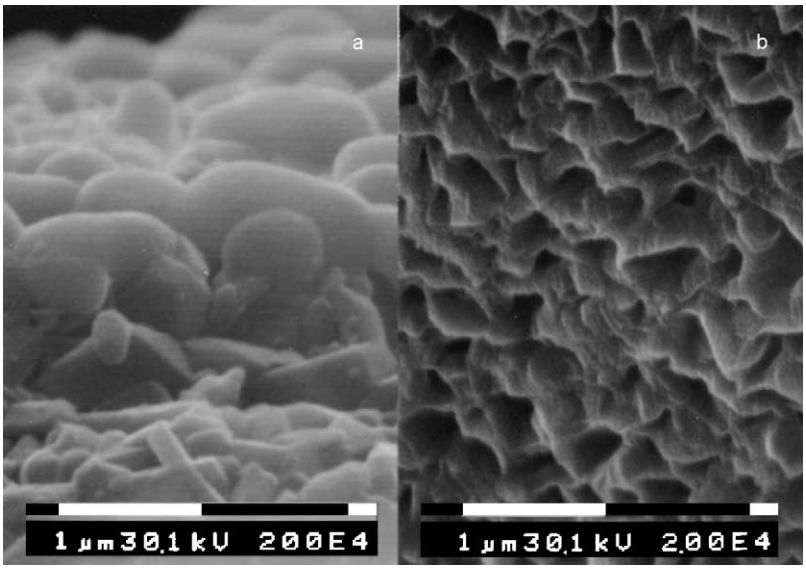

Fig. 1. SEM micrographs of different morphologies of the α-alumina layer covering the FeCrAlloy fibres: (a) 900 °C, 1 h in still air; (b) 1200 °C, 5 min at 0.5% O_2 in nitrogen.

suitably optimised. At 1200 °C for 5 min in a lean oxygen atmosphere (0.5 vol.% in nitrogen) it was possible to obtain an α-alumina layer with sharp and elongated grains (Fig. 1). Such an optimised alumina layer structure enabled both a strong adhesion with the basic alloy and a very rough external surface, but offers only a fair specific surface area (2–3 m^2/g) for the direct dispersion of Pd clusters.

2.2. The catalysts: preparation, characterisation and catalytic activity testing

Owing to the low surface area of the α-alumina layer covering the metal fibre panels, Pd was dispersed over γ-alumina, a high BET surface area carrier. This material was tentatively selected to provide both good adhesion and chemical affinity with the α-alumina coating of the pre-oxidised FeCrAlloy mat. As a first step, transition alumina powders were prepared via a *combustion synthesis* technique, that can yield in short times to a fine and homogeneously dispersed product [22,23]. With this technique, γ-alumina can be rapidly prepared starting from a solution of the aluminum nitrate precursor (the oxidant) and urea (the fuel) heated at low temperature (less than 600 °C) by an external source, to ignite the straightforward and highly exothermic reaction. The fast self-propagating reaction wave leads in few seconds to the final product, the oxide, in a foamy and brittle state [22]. By varying the starting mixture composition and the synthesis temperature the dynamics of the process can be influenced leading to different tailored microstructures and properties of the aluminum oxide.

A high specific surface area alumina could be synthesised starting from an understoichiometric urea/aluminum nitrate mixture heated up to 500 °C, according to the procedures described in Ref. [24]. In order to stabilize such a γ-alumina different amounts of lanthanum (as lanthanum nitrate) were added to the starting solution. A number of samples were aged at various temperatures, up to 1100 °C and characterised, measuring the BET surface area and evaluating the crystalline structure by X-ray diffraction.

The deposition of a different palladium loading (1–8 wt.% of Pd) over the high-surface alumina, previously crushed into 80–180 μm powder granules, was carried out according to an incipient wetness impregnation with aqueous solution of $Pd(NO_3)_2$. The catalysts were dried overnight at 120 °C and calcined at 500 °C for 2 h in still air to allow a good PdO dispersion over the carrier. In each case, palladium was present as PdO, as determined by thermal gravimetric

analysis (TGA) decomposition and temperature-programmed reduction (TPR) experiments. Hydrogen reduction, carried out at 400 °C, yield finally to the formation of small clusters of metallic Pd [15]. With the aim to minimize the changes in particle size that would occur during high temperature combustion, the catalyst was stabilised at 1000 °C in oxygen for 8 h.

The catalytic activity of the Pd/alumina catalysts towards methane oxidation was evaluated by temperature-programmed combustion (TPC). Approximately, 0.1 g of fresh catalyst was mixed with a silica wool and loaded into a fixed bed quartz tubular reactor with a 3 mm internal diameter. The reactor was placed into an electric oven equipped with an automatic temperature controller and was fed with a reaction mixture of 2% methane, 16% oxygen in helium at 50 ml/min, controlled by mass flow meters (Brooks). The reaction products were analysed by using continuous analysers (URAS14 by Hartmann and Braun) thereby obtaining the concentration values of methane, carbon dioxide, carbon monoxide and oxygen. The TPC outlet concentration profiles of all these compounds were recorded at a 5 °C min^{-1} cooling rate.

2.3. The catalytic burners: preparation and testing

The metal fibre panels A, B and C were washcoated with Pd/alumina powders (2 wt.% Pd on the La-promoted γ-alumina obtained by combustion synthesis). A slurry was obtained by ball-milling a mixture of the Pd/alumina with a common binder (methyl cellulose) in a dilute nitric acid solution. The metal panels were coated by several dipping and drying cycles, in order to get a Pd/alumina loading of about 2 wt.% referred to the overall weight of the three burners. A final calcination at 1000 °C for 12 h was performed to stabilise the catalyst.

The three catalysed flat burners (160 mm × 250 mm) were tested in a combustion chamber (maximum input power: 30 kW) fed with natural gas. The apparatus was described elsewhere [10]. Briefly, the mass flow rates of gas and air were separately controlled by means of an electrovalve and a fan, respectively, and fed through a Venturi mixer. The air–gas mixture was delivered to the premixed chamber where a series of two plates, a diverter and a perforated plate, homogenised the velocity profile all over the burner surface, in order to prevent from flame instabilities. Each burner was horizontally fitted at the bottom of the combustion chamber and fired upwards to a 'finned-tube' type heat exchanger fitted at the top. An alumina fibre mat was employed as an additional burner under-layer to prevent flashback. Once the burner was spark-ignited, it fired upwards and the exhaust gases were dispersed in the atmosphere through a chimney. Quartz windows on the walls of the combustion chamber allowed internal inspection of the burner unit.

Tests were carried out in the power input range 150–750 kW/m^2 at different excess air values, 2–80%. The composition of the exhaust gases was analysed through a set of continuous analysers to detect the NO, CO, and CO_2 (URAS14-H&B NDIR analysers) and O_2 concentrations (MAGNOS16-H&B paramagnetic oxygen analyser). The upper (burnerdeck) and lower (mixture inlet side) surface temperatures, at the central location of the rectangular burner, were recorded during each test. The temperature measurements were performed by means of K-type thermocouples.

3. Results and discussion

3.1. The Pd alumina catalyst

The combustion synthesis method was successfully applied in order to get a high-surface area transition alumina. Up to now, reference literature data refer only to nanosized α-aluminas, synthesized by the combustion of aqueous solutions containing aluminum nitrate, ammonium nitrate and glycine [25,26]. In this work, urea/aluminium nitrate/lanthanum nitrate mixtures were used. Due to the combustion of natural gas, the high temperatures (even higher than 1000 °C) as well as the generation of large amounts of water may force the irreversible transformation of γ-alumina towards the more thermodynamically stable α-alumina [27,28], whose crystallization is accompanied by specific surface area and pore volume decrease, that often cause the encapsulation of the active component with permanent loss of catalytic activity [29]. Lanthanum was selected as an anti-sintering dopant [30–33], since it is generally recognised as a valid hydrothermal stabilizer of high-surface area transition alumina especially, when active species as Pd or Pt are deposited on it [34,35].

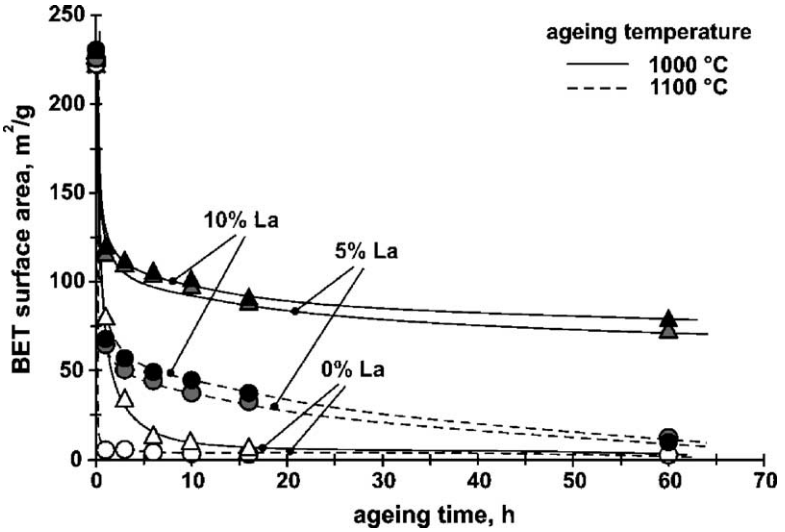

Fig. 2. Influence of thermal ageing on BET specific surface area of alumina powders, prepared by the combustion synthesis technique and stabilised with different amount of lanthanum. Ageing temperatures: 1000 and 1100 °C.

The effect played by a different amount of lanthanum on alumina powders prepared according to the previous combustion synthesis procedure is shown in Fig. 2, where the BET specific surface area of fresh and aged alumina is reported. The fresh alumina provides a very high BET surface area (>220 m^2/g), almost independently of the lanthanum content. However, XRD patterns put into evidence some impurities, due to the presence of some carbonaceous residues derived from the organic precursors. After a 1 h calcination at 800 °C, the complete crystallisation of γ-alumina without significant impurities was confirmed by XRD analysis. Particularly, Fig. 2 provides evidence that a 5 wt.% of lanthanum is sufficient to keep high and almost stable the BET surface area, even after prolonged exposure at high temperature. After 6 h at 1000 °C, for instance, the BET surface area of the doped alumina decreased to 80 m^2/g, while at the same time the BET surface area of the non-promoted alumina fell down to 5 m^2/g. X-ray diffraction analysis of the aged samples, on the one hand, confirmed that, the pure aluminas evolved towards the irreversible α-form, on the other hand, it revealed that the promoted alumina could survive as the γ-form together with some surface $LaAlO_3$ perovskite. As generally recognised [36,37], in the $LaAlO_3$ perovskite, the Al^{3+} ion preferentially occupies the octahedral site, rather than the less stable tetrahedral one, as typical of transition aluminas. The aluminum ions result blocked into a thermally stable perovskite, located in surface micro-domains, providing a certain rigidity to the structure and preserving from sintering. XRD patterns of the modified alumina, aged at temperatures higher than 1050 °C, revealed a change in the crystal structure. Under severe ageing, in fact, the $LaAlO_3$ perovskite progressively disappeared by solid state reaction with alumina forming the so-called lanthanum β-Al_2O_3 structure (corresponding to $La_2O_3{\cdot}nAl_2O_3$ with n in the range 11–14). A severe drop of area occurred along with the appearance of the lanthanum β-Al_2O_3 phase, which reduced the effect of $LaAlO_3$ perovskite and entailed a subsequent sintering of alumina crystals and the irreversible transition towards the a form.

In agreement with some authors [38], notwithstanding a 5 wt.% La resulted almost sufficient to guarantee a good thermal stability of the transition alumina, a 10 wt.% of the dopant was considered. Although an increase in the dopant content (up to 10%) does not lead to any particular improvement, such a relatively high content is indeed generally indicated to increase the PdO-decomposition temperature to over 900 °C and to provide structural oxygen to palladium [39].

The influence of the palladium loading (0.5, 1, 2, 4, and 8 wt.%) on alumina on the catalytic activity

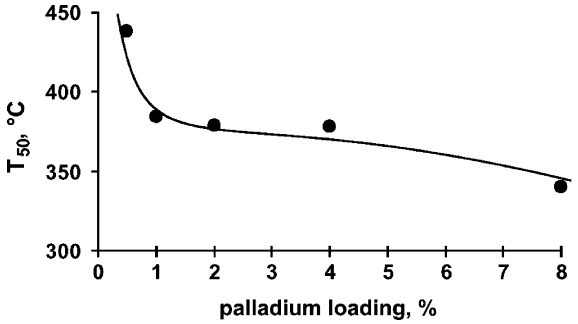

Fig. 3. Influence of the palladium loading on the catalytic activity, evaluated according to TPC testing and expressed as T_{50} (methane half conversion temperature).

towards methane combustion was investigated by carrying out specific TPC tests. Fig. 3 shows the 50% methane conversion temperature (T_{50}) obtained for different Pd loadings. Similar trends, here omitted, were found for T_{10} and T_{90} (corresponding to 10 and 90% methane conversion, respectively). As the palladium loading was increased from 0.5 to 1 wt.% the methane conversion resulted further improved (from $T_{50} = 438$ to 384 °C). At 1–4 wt.% palladium, no significant increase of catalytic activity could be observed (T_{50} remained almost constant at about 380 °C). The amount of palladium, in fact, had to be enhanced up to 8 wt.% in order to yield a certain benefit for the catalytic activity (T_{50} decreased to 340 °C). Even if 1 wt.% seems to be sufficient to guarantee a satisfying catalytic activity, taking into account that Pd is very expensive, a loading of about 2 wt.% was provisionally considered as the best compromise between performances and costs.

3.2. The preparation of catalytic burners

The so prepared Pd/alumina catalyst was then washcoated onto the three metallic fibre burners A, B and C. Process variables were determined to obtain a good catalyst suspension in the slurry and uniform catalyst coating over the fibres. The catalysed fibre burners were dried and then calcined in air, to result in a high-surface area of exposed metallic palladium. The deposition of the catalyst was highly homogeneous through all the burner thickness. As shown in Fig. 4, one can differentiate among the FeCrAlloy core, the α-Al_2O_3 layer and the Pd-alumina catalyst, uniformly dispersed in fine aggregates.

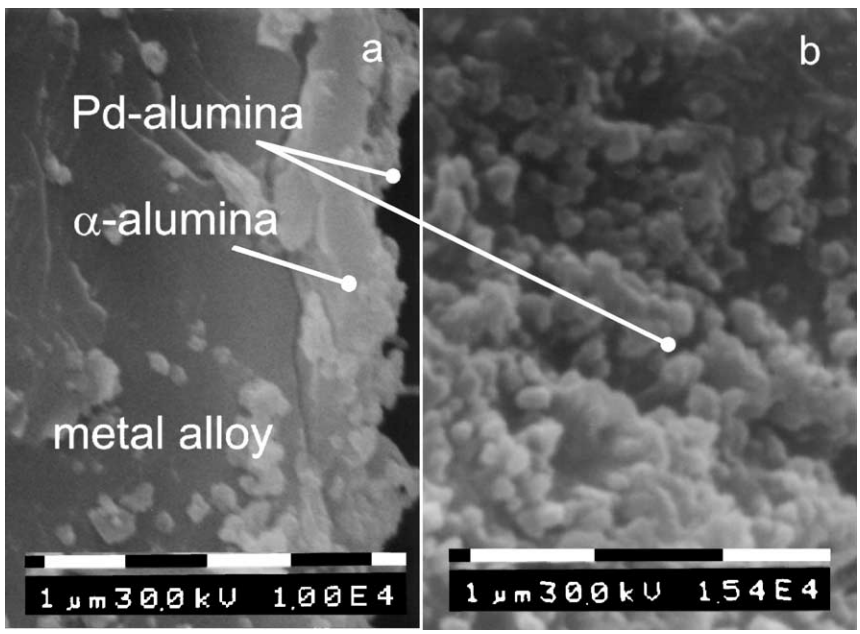

Fig. 4. SEM micrographs of a Pd/alumina catalysed fibre: (a) cross-section; (b) surface.

In order to verify the degree of catalyst anchoring to the fibres, additional vibration tests evidenced that just some short pieces of the fine fibres could be lost, exactly as occurred in the absence of the catalyst. Conversely, a negligible amount of fine catalyst powder was lost, which confirmed the strong and satisfactory adhesion of the catalyst to the metal fibres.

3.3. Tests on catalytic and non-catalytic burners

Initial screening tests were performed on the six burners considering both the catalysed and the non-catalysed ones. The goal of these tests was to determine the most promising catalytic burner, and to carry out additional tests with this latter. The initial and extensive campaign of tests was performed by varying the input power (150–750 kW/m^2) and the excess air values (2–70%).

Primarily, it has to be outlined that the catalytic burner C could not guarantee the same large field of stable and steady combustion as the other two burners; a steady combustion process, in fact, could not be maintained for excess air values lower than 12%, whatever the input power was. Fig. 5 reports a sequence of images that illustrate the unstable behaviour of such catalytic burner when operated at an excess air of about 10% and a specific power input of about 375 kW/m^2. At low Q and E_a values, the catalytic burner was affected by an anomalous phenomenon: the radiant output progressively increased with time, as confirmed by the enhanced brightness of the firing surface (Fig. 5a–c). Contemporarily, some dark zones, characterised by a lower temperature, appeared and stabilised here and there over the burnerdeck. Only after about 15–90 s (depending on the excess air ratio) such dark zones rapidly disappeared, leading to a uniformly bright firing burner (Fig. 5d). This last operating condition was though immediately followed by combustion extinction due to flashback (Fig. 5e). Such a thermal instability has likely to be attributed to the nature of the Pd catalyst, as it cannot be observed on the non-catalytic burner and it was never observed with the perovskite-catalysed burners previously examined [8–10].

However, the Pd/alumina catalyst, known as an excellent candidate for methane combustion, enabled the stabilization of the combustion process deeper inside the burner, as indicated by the enhanced brightness (Fig. 5c). Unfortunately, when the momentum of the reacting gases is too low (low Q and E_a values), such occurrence leads easily to flashback, since thermal conductivity of the burner forces the reaction zone backward until it reaches the plenum chamber (Fig. 5e). It is thus not surprising that burner C, characterised by a high fibre density (i.e. higher thermal conductivity and higher surface area of catalyst exposed

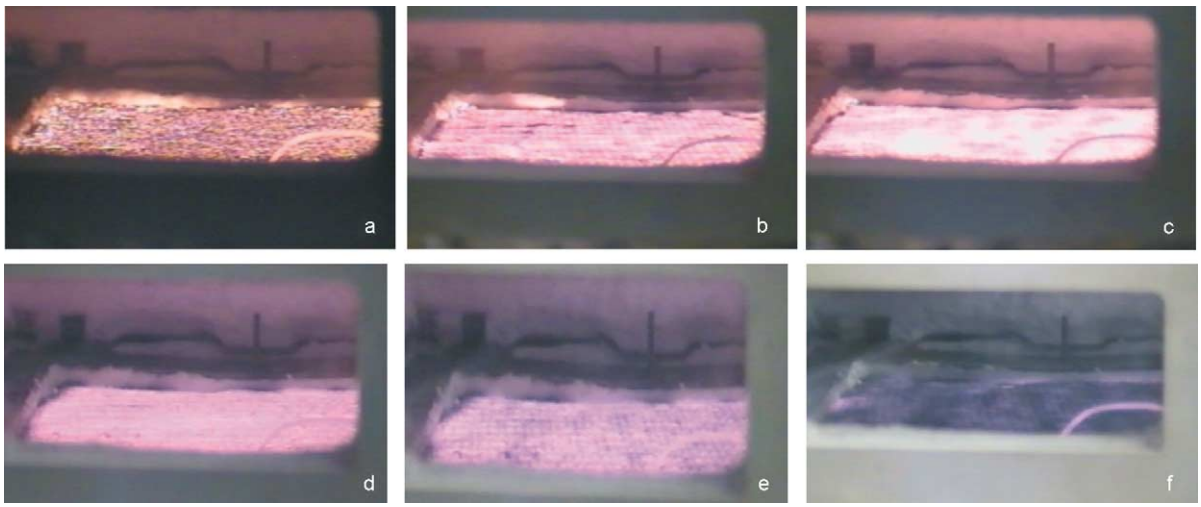

Fig. 5. Sequence of video images of the Pd/alumina catalysed burner C fired at 375 kW/m^2 and 10% of excess air at different time steps from ignition: (a) 1–3 s, (b) 8–26 s, (c) 27–28 s, (d) 28 s, (e) 29 s, and (f) 30 s.

to the reacting mixture) was the only one affected by flashback and flame instability problems.

As far as the pollutant emissions are concerned, the CO and NO concentrations, generated at three specific input powers (about 240, 430, and 700 kW/m^2), by the Pd-catalysed burners A, B and C are reported in Fig. 6a–c, respectively; the unburned HC were always practically undetectable.

The NO levels results higher, as the input power was increased up to the conditions typical of the blue-flame regime, where the flame temperature could not be quenched by the porous medium, generally acting as a conductive and radiant sink. By decreasing the excess air, there was a sort of competition between the higher contact time between the oxygen and nitrogen species, and the lower oxygen partial pressure. The two variables play from opposite sides on the NO generation [40] leading more often to higher NO levels. By comparing the NO emissions produced by the three catalytic burners, no significant differences can be really observed. If burner A produced lower NO levels at 700 kW/m^2, burner B guaranteed better limits at power $<$240 kW/m^2. Burner C, as explained before, could not operate for excess air lower than 12%. Anyway, at about 15–20% of excess air, normally adopted in practical applications, all the three burners generated similar NO concentrations, about 30–37 ppmv.

As regards the CO levels, the higher concentrations were observed at low excess air, where the reduced oxygen partial pressure can be a limiting factor for the conversion of CO into CO_2. Once again, the three catalysed burners could guarantee extremely good and similar performances when working at excess air of about 15–20%; the CO concentrations, in fact, resulted always lower than about 40 ppmv.

All the three catalysed burners always guaranteed better performances both in terms of CO and NO emissions than their respective non-catalytic counterparts. Among the three catalytic burner, if a choice has to be taken, burner B has to be preferred. On the one hand, burner C suffered from a lower stable operation range, whereas burner A for its low fibres density and mat thickness could provide a lower durability, with respect to the other two types. To provide evidence of the improvement provided by the dispersion of the Pd/alumina catalyst, a comparison between the general performances of the burners B, both catalysed and not, are hereafter considered.

To gain a better understanding of the recorded emissions, it is important to correlate those to the combustion regimes stabilizing at each operating conditions. Fig. 7 shows the map of the combustion regimes for both the catalytic and the non-catalytic burner. Particularly, as regards the Pd-catalysed burner, the additional dotted line delimits the region where on the radiating burner surface there was the appearance and the disappearance of some small opaque zones. By comparing the extension of the radiant regime of the two burners, an opposite behaviour can be remarked: for specific powers lower than about 380 kW/m^2, the Pd-catalysed burner could maintain a flameless combustion for excess air levels higher than those of the non-catalytic burner, while, for specific powers higher than 380 kW/m^2, the Pd-catalysed burner shifted into the transition regime at excess air values lower than those of the non-catalytic one. This behaviour is related to the combination of two opposite phenomena, whose importance changes depending on the operating conditions:

(1) The deposition of the catalyst over the metal fibres reduces both the porosity and the pore size of the burner and increases the gas path tortuosity. This enhances the local gas momentum which tends to push the flame outside the burner.
(2) The catalyst could help in stabilising the flame front at least partly inside the porous medium by promoting hetero–homogeneous reactions in the gas phase via free radicals generation (e.g. OH$^\bullet$).

At high powers ($>$380 kW/m^2), the configuration of the burner surface easily changed from the flameless to the transition to the blue-flame mode by increasing the excess air mainly due to effect 1. On the other hand, when operating at low powers ($<$380 kW/m^2) the methane combustion resulted in being more catalytically assisted (effect 2), as a consequence of higher residence times in the burner, and an increase in the air-to-fuel did not lead immediately to a shift into the transition or the blue-flame regime.

As an indirect evaluation of the burner surface radiosity, optical direct observation and temperature measurements were considered. Fig. 8 shows the temperatures measured at the central position over the firing surface versus the specific power, at different excess air values. The Pd-catalysed burner, whatever were the operating conditions, resulted in being hotter

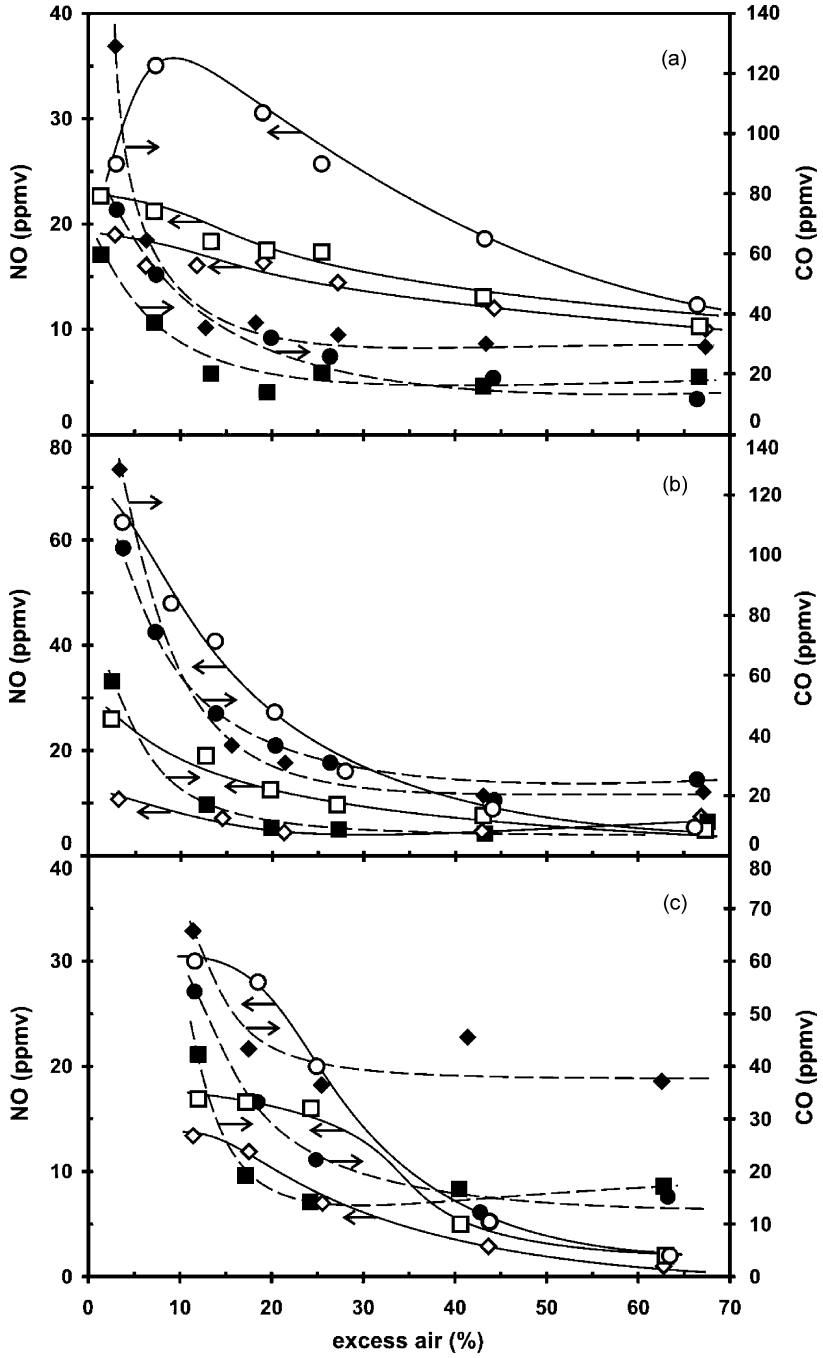

Fig. 6. CO (empty symbols) and NO (black symbols) emissions (dry flue gases, 0 °C and 1013 mbar) versus the excess air at three specific powers for (a) burner A, (b) burner B, and (c) burner C. Legends: (◇, ◆) 240, (□, ■) 430, and (○, ●) 700 kW/m^2.

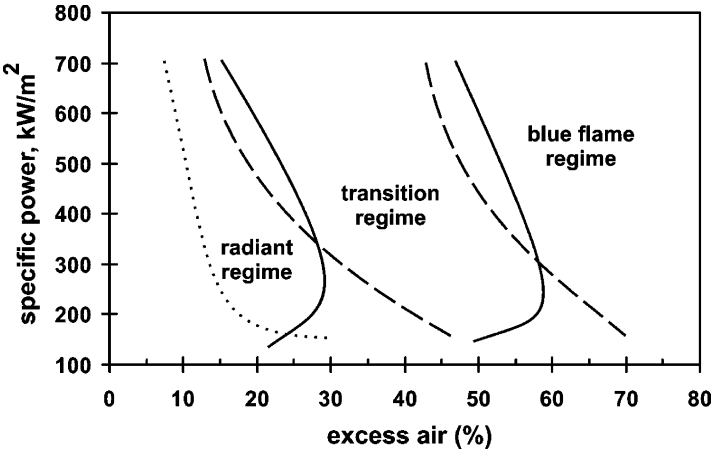

Fig. 7. Combustion regimes map for both the non-catalytic (solid lines) and Pd/alumina catalysed (dashed lines) burners B. The dotted line delimits the region, within the radiant regime, where a non-homogeneous temperature distribution affected the catalytic burner surface.

than its catalyst-free counterpart. The Pd catalyst, as already reported, in addition to the surface heterogeneous mechanisms, that are limited at high temperatures because they are mass-transfer controlled, can promote the homogeneous gas phase reactions, by the generation of free radicals. If a greater amount of the combustion heat is thus released within the porous medium, its surface temperature increases to the benefit of the radiant output. By the way, as the radiant output increases, the amount of energy lost by convection of the cold flue gases decreases, enhancing the overall thermal efficiency of the combustion system.

If the catalyst stabilizes the combustion reactions deeper inside the burner, the homogeneous gas phase is cooled by the porous medium that absorbs and radiates part of the released heat. The lower the flame temperatures the lower the NO emissions generated according to the thermal Zeldovich mechanism [40,41]. Such considerations find a confirmation in Fig. 9, where the Pd-catalysed burner guaranteed NO levels lower than those produced by the non-catalytic

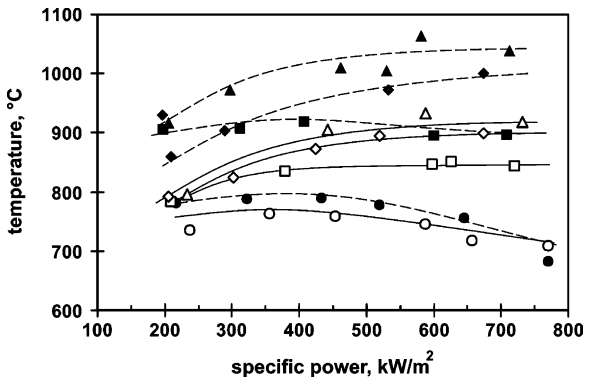

Fig. 8. Burner surface temperature measured over both the non-catalytic (empty symbols) and Pd/alumina catalysed (black symbols) burners B versus the specific powers at different excess air. Legends: excess air, (△, ▲) 2%, (◇, ◆) 14%, (□, ■) 26%, and (○, ●) 43%.

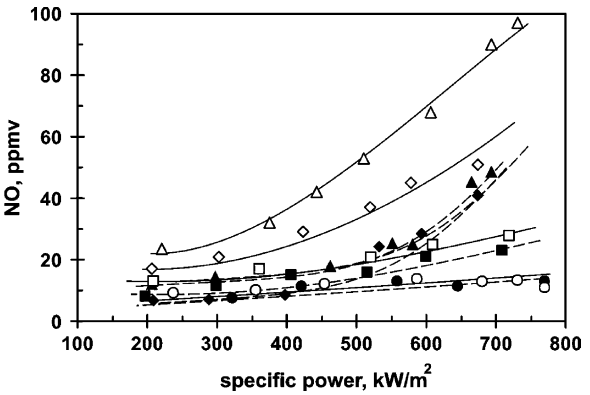

Fig. 9. NO emissions for both the non-catalytic (empty symbols) and Pd/alumina catalysed (black symbols) burners B versus the specific powers at different excess air. Legends: excess air, (△, ▲) 2%, (◇, ◆) 14%, (□, ■) 26%, and (○, ●) 43%.

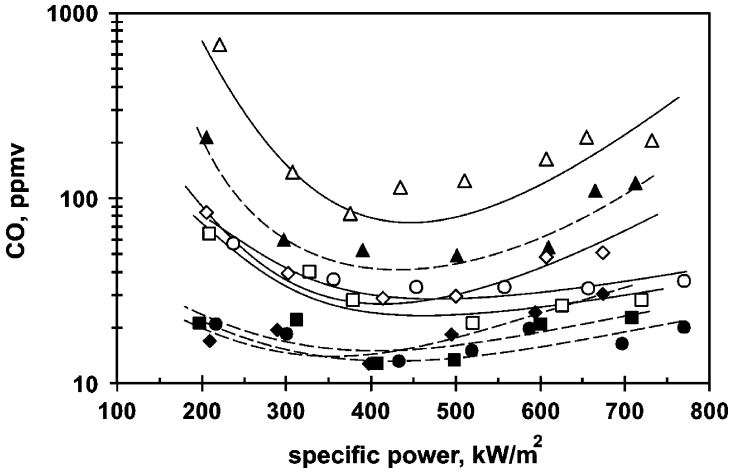

Fig. 10. CO emissions for both the non-catalytic (empty symbols) and Pd/alumina catalysed (black symbols) burners B versus the specific powers at different excess air. Legends: excess air, (△, ▲) 2%, (◇, ◆) 14%, (□, ■) 26%, and (○, ●) 43%.

one. This phenomenon resulted more evident for low values of the excess air, where the flame temperature is the controlling factor of NO formation. At excess air of about 2–3%, approximating the stoichiometric conditions, the catalyst could decrease the NO emissions of about 50% with respect to the absolute value of the non-catalytic burner, whatever the input power was. For instance at 700, 400 and 350 kW/m^2, the catalyst decreased the NO levels from 90 to 48 ppmv, 40 to 18 ppmv and 24 to 13 ppmv, respectively.

In order to provide a complete explanation of the differences between the two burners of type B, the Pd-catalysed and the non-catalytic one, Fig. 10 shows the CO levels obtained. Once again the presence of the catalyst promoted the selectivity of methane towards the CO_2 product, reducing the CO levels. At air-to-fuel ratios approaching the stoichiometric conditions, the non-catalytic combustion was strongly penalised, while the catalyst could decrease the unacceptable emissions to lower values. At excess air of about 15–25%, the catalyst decreased the CO emissions in the whole range of the input power to maximum values lower than about 30 ppmv, whereas the non-catalytic burner produced CO levels up to about 90 ppmv.

Some final remarks have to be addressed to a peculiar phenomenon encountered when shifting rapidly the excess air value from high to low values and back, at low specific power inputs. Fig. 11 refers to the CO outlet concentration registered at 400 kW/m^2 when shifting the excess air E_a from 90% down to only 2% and then back to 95%. The above high E_a values were selected on purpose to let the surface temperature of the burner to reach a value as low as 500 °C, well below the Pd-to-PdO transition temperatures [42]. Conversely, the 2% E_a value was fixed to reach temperatures higher than 950 °C thereby forcing PdO to transform into Pd [43].

As opposed to what happens with non-catalytic burners, each time the gas feed is changed CO emissions progressively decrease, which is thus a likely

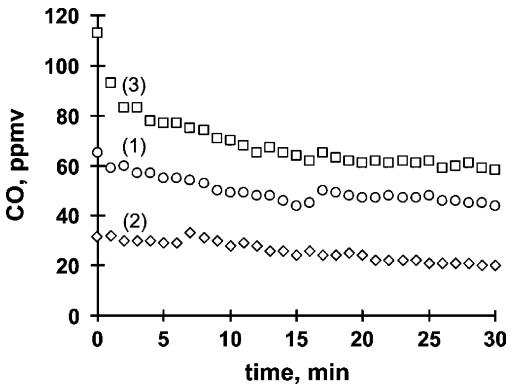

Fig. 11. Time variation of the Pd/alumina catalysed burner performance, expressed in terms of CO emissions at 400 kW/m^2 and at three different E_a values: (1) 90%, (2) 2–3% and (3) 95%.

consequence of the presence of the Pd catalyst and likely to its phase transformations. It was observed [43] that such a transition can last from some minutes up to some hours, depending on the working temperature and the oxygen partial pressure. Particularly, it was demonstrated that the PdO-to-Pd transformation has a higher rate than the backward reaction, and at high temperatures the metal form is the more stable one.

Coming back to the data plotted in Fig. 11, it can be that, the particularly sharp decrease of CO outlet concentration observed during run 3 can be ascribed to slow transformation of Pd to the more active PdO species on the grounds of the high oxygen concentration levels ($E_a = 95\%$) and of the comparatively low temperature (about 500 °C). During run 2, in fact, the combination of high temperatures and low oxygen concentration occurring over the downstream part of the burner should have led rapidly to formation of Pd, which is less active at moderate temperatures [15,17,19,36]. When E_a was set back to 95% the increased momentum of the reacting gas mixture pushed the reaction front outside the burner which got colder. The only catalyst that could play a role on the combustion process in these new operating conditions was the one placed on the downstream part of the burner, exactly where the previous operating conditions (run 2) caused the formation of the less active Pd. As a consequence, the initial CO emissions turned out to be rather high at the beginning of run 3, but then, as long as the Pd-to-PdO transformation occurred, they decreased significantly. These Pd/PdO phase changes are likely to affect also the stability of the catalytic burners, as hypothesised before when dealing with the unsteady behaviour of burner C.

Finally, one should not be surprised of the comparatively low CO value observed during run 2. It should in fact be due to the high residence time of the flowing gases in the catalytic burner. On the one hand this should entail that the hot downstream burner fibres should be characterised by a rapid shift of PdO to the less active Pd. On the other hand, however, owing to the homogeneous catalyst distribution throughout the burner thickness, inner and colder burner fibres characterised by the presence of the more active PdO phase will always be available to sustain the combustion process. Furthermore, recent studies [43] show that Pd seems to be more active than PdO at high temperatures as those typical of the hot downstream burner surface.

4. Conclusions

The primary goal of the present contribution was the development of a catalytic pre-mixed fibre burner for household applications, characterised by a markedly lower environmental impact in terms of NO_x, CO and HC, compared to their non-catalytic counterparts. The deposition of the Pd-alumina catalyst over several Fe-CrAlloy fibre mats was accomplished via washcoating with ad hoc developed Pd catalysts dispersed on La doped γ-Al_2O_3. All catalytic burners stabilised the combustion process more inside the porous burner matrix, thereby maximising the heat fraction transferred by radiation (increasing the efficiency), cooling the flame temperature (reduced NO emissions) and improving the combustion completeness (lower levels for CO and unburned HC). Some flame instability phenomena were though noticed for the denser catalytic fibre mat structures, leading eventually to flashback at low specific power inputs and excess air values. Furthermore, the Pd-to-PdO transition was found to affect the dynamic behavior of the catalytic burners.

Long-term tests are now being carried out under accelerated ageing conditions in order to assess the burners reliability (target of 30 000 operating hours under practical operating conditions), a pre-requisite for the domestic boiler applications.

Acknowledgements

Funding of the European Union is gratefully acknowledged (EU project HIMOCAT: High-modulation, high-efficiency and low-emission boilers for household application based on pre-mixed catalytic burners). The complimentary supply of burners by NV Acotech SA (Zwevegem, Belgium; http://www.acotech.com) is also kindly acknowledged.

References

[1] Kyoto Protocol to the United Nations Framework Convention on Climate Change, English conference of the parties, Third session Kyoto, December 1–10, 1997.

[2] K.J.A Hargreaves, H.R.N. Jones, D.B. Smith, Developments in Burner Technology and Combustion Science, in: Proceedings of the 52nd Autumn Meeting of Institution of Gas Engineers, Comm. No. 1309, November 12, 1986, London, pp. 1–31.
[3] R. Viskanta, J.P. Gore, in: Proceedings of the Fourth International Conference on Technologies and Combustion for a Clean Environment, Lisbon, 1997;
R. Viskanta, J.P. Gore, in: Proceedings of the Third ASME/JSME Joint Thermal Engineering Conference, Lisbon, 1997.
[4] V. Khanna, R. Goel, J.L. Ellzey, Comb. Sci. Technol. 99 (1994) 133.
[5] S.B. Sathe, R.E. Peck, T.W. Tong, Comb. Sci. Technol. 70 (1990) 93.
[6] J.D. Sullivan, 1991, Basic research on radiant burners, Semi-Annual Report (July 1991), GRI Report No. 91/0331, Santa Clara, CA.
[7] G. Saracco, S. Sicardi, V. Specchia, R. Accornero, M. Guiducci, M. Tartaglino, Gaswärme Int. 45 (1996) 24.
[8] G. Saracco, I. Cerri, V. Specchia, R. Accornero, Chem. Eng. Sci. 54 (1999) 3599.
[9] I. Cerri, G. Saracco, F. Geobaldo, V. Specchia, Ind. Eng. Chem. Res. 39 (2000) 24.
[10] I. Cerri, G. Saracco, V. Specchia, D. Trimis, Chem. Eng. J. 82 (2001) 73.
[11] S. Moßbauer, O. Pickenäcker, K. Pickenäcker, D. Trimis, in: Proceedings of the Fifth International Conference on Technologies and Combustion for a Clean Environment, Lisbon, 1999.
[12] J.A. Eng, D.L. Zhu, C.K. Law, Comb. Flame 110 (1995) 645.
[13] B.H. Chao, Y.Q. Xia, Comb. Flame 121 (2000) 625.
[14] R.B. Anderson, K.C. Stein, J.J. Feenan, L.E.J. Hofer, Ind. Eng. Chem. 53 (1961) 809.
[15] R.J. Farrauto, J.K. Lampert, M.C. Hobson, E.M. Waterman, Appl. Catal. B 6 (1995) 263.
[16] L.M. Quick, S. Kamitomai, Catal. Today 26 (1995) 303.
[17] J.C. McCarty, Catal. Today 26 (1995) 293.
[18] E. Kikuchi, T. Matsuda, N. Takahashi, in: Proceedings of the Symposium on catalytic combustion, San Francisco, Am. Chem. Soc. Div. Pet. Chem. 42 (1) (1997) 146.
[19] R. Burch, Pure Appl. Chem. 68 (1996) 377.
[20] C. Badini, F. Laurella, Surf. Coat. Technol. 135 (2001) 291.
[21] Brite-Euram project LIFEBURN, Development of a lifetime prediction method to improve the design of premixed radiant burners for domestic applications, 1997–2001.
[22] J.J. Kingsley, K.C. Patil, Mater. Lett. 6 (1988) 427.
[23] S.R. Jain, K.C. Adiga, Comb. Flame 40 (1981) 71.
[24] A. Civera, M. Pavese, G. Saracco, V. Specchia, Catal. Today 83 (2003) 199.
[25] T. Mimani, K.C. Patil, Mater. Phys. Mech. 4 (2001) 134.
[26] K.C. Patil, S.T. Aruna, S. Ekambaran, Curr. Opin. Solid State Mater. Sci. 2 (1997) 158.
[27] D.L. Trimm, in: C.H. Bartolomew, J.D. Butt (Eds.), Catalyst Deactivation, Vol. 29, Elsevier, Amsterdam, 1991.
[28] H. Arai, Appl. Catal. A 138 (1996) 161.
[29] H. Arai, M. Machida, Catal. Today 10 (1991) 81.
[30] M. Michel, R. Poisson, French Patent 2 257 335.
[31] M. Michel, R. Poisson, French Patent 2 290 950.
[32] H. Schaper, E.B.M. Doesburg, L.L. Van Reijen, Appl. Catal. 7 (1983) 211.
[33] I.M. Tijburg, H. De Bruin, P.A. Elberse, J.W. Geus, J. Mater. Sci. 26 (1991) 5945.
[34] F. Oudet, P. Courtine, A. Vejeux, J. Catal. 114 (1988) 112.
[35] A. Miller, J. Appl. Phys. Suppl. 30 (1959) 245.
[36] B. Beguin, E. Garbowski, M. Primet, Appl. Catal 75 (1991) 119.
[37] P. Euzen, J.-H. Le Gal, B. Rebours, G. Martin, Catal. Today 47 (1999) 19.
[38] A.G. Errson, E.M. Johansson, S.G. Järås, in: B. Delmon, P.A. Jacobs, R. Maggi, J.A. Martens, P. Grange, G. Poncelet (Eds.), Studies in Surface Science and Catalysis, Preparation of Catalysts VII, Louvain-La-Neuve, Elsevier, Amsterdam, 1998, p. 601.
[39] E.M. Johansson, K.M.J. Danielsson, E. Pocoroba, E.D. Haralson, S.G. Järås, Appl. Catal. A 182 (1999) 199.
[40] J.A. Miller, C.T. Bowman, Prog. Energy Comb. Sci. 15 (1989) 287.
[41] A.A. Siddiqi, J.W. Tenini, Hydrocarbon Processing, vol. 60, October 1981 issue, p. 115.
[42] G. Groppi, C. Cristiani, L. Lietti, P. Forzatti, Stud. Surf. Sci. Catal. 130 (2000) 3801.
[43] M. Lyubovsky, L. Pfefferle, Catal. Today 47 (1999) 29.